ChemComm

COMMUNICATION

View Article Online
View Journal | View Issue

Cite this: *Chem. Commun.*, 2023, 59, 5918

Received 16th January 2023,
Accepted 12th April 2023

DOI: 10.1039/d3cc00243h

rsc.li/chemcomm

Mixed noble metal–oxo clusters: platinum(IV)–gold(III) oxoanion $[Pt^{IV}_2Au^{III}_3O_6((CH_3)_2AsO_2)_6]^-$†‡

Jiayao Zhang, [a] Saurav Bhattacharya, [ab] Anja B. Müller, [a] Levente Kiss, [c] Cristian Silvestru, [c] Nikolai Kuhnert [a] and Ulrich Kortz *[a]

The first discrete mixed platinum(IV)–gold(III) oxoanion $[Pt^{IV}_2Au^{III}_3O_6((CH_3)_2AsO_2)_6]^-$ (1) was synthesized by reaction of $H_2Pt(OH)_6$ with $H[AuCl_4]$ in a simple one-pot procedure in aqueous solution at pH 7 and comprises two equivalent $Pt^{IV}O_6(As(CH_3)_2)_3$ units which are linked by three square-planar $Au^{III}O_4$ units. Polyanion 1 could be isolated as a potassium or sodium salt in good yield, which were structurally characterized in the solid state by single-crystal XRD and TGA, and in solution by multinuclear (^1H, ^{13}C, ^{195}Pt) NMR, indicating that polyanion 1 is stable in solution, which was confirmed by ESI-MS studies. The sodium salt of 1 undergoes a clean single-crystal-to-single-crystal (SCSC) structural transformation upon rehydration and dehydration.

Polynuclear coordination complexes form a large and diverse class of inorganic compounds, and anionic metal–oxo clusters known as polyoxometalates (POMs) form an important subclass.[1] The enormous structural and compositional diversity and associated unique combination of different physicochemical properties of POMs have had an impact in many areas of chemistry, material science, medicine, and catalysis.[2] Classical POMs comprise early d-block metal ions in high oxidation states (*e.g.* W^{VI}, V^V) as addenda and mainly edge- and corner-shared MO_6 octahedra as structural motifs. The incorporation of noble metals such as Pt, Pd, and Au in lacunary POMs has attracted extensive attention, not only due to structural features, but the combination of the catalytic properties of the noble metals with the ability of the POM fragment to act as a thermally stable, soluble and redox-active host, relevant for catalytic intermediates in numerous industrially relevant processes and devices, including easily accessible "green" H_2O_2/O_2-based oxidations.[3]

In 2004, the first noble metal oxoanion, $[Pt^{III}_{12}O_8(SO_4)_{12}]^{4-}$, was reported by Wickleder's group and this species is composed of six dumbbell-shaped metal–metal bonded Pt^{III}_2 dimers coordinated by oxo and sulfato bridges,[4a] and recently the first polythioplatinate(II), $[Pt^{II}_3S_2(SO_3)_6]^{10-}$, was reported by our group.[4b] The first member of a polyoxopalladate(II), $[Pd^{II}_{13}As_8O_{34}(OH)_6]^{8-}$ ($Pd_{13}As_8$), was discovered by our group in 2008 and this anion comprises a cuboid-shaped assembly with one central and 12 external Pd^{II} ions in a square-planar coordination geometry, and eight arsenato capping groups.[5] To date, more than 80 polyoxopalladates(II) with a large compositional and structural variety (*e.g.* cube, star, bowl, dumbbell, wheel, and open-shell archetypes) have been prepared by using various external capping groups RXO_3^{n-} (X = P^V, As^V, Se^{IV}, V^V; R = O, Ph, lone pair) and many different central metal ion guests M (M = s, p, d or f element).[3b] Recently, we reported the first examples of neutral palladium(II)–oxo clusters (POCs), $[Pd_{16}O_8(OH)_8((CH_3)_2AsO_2)_8]$ (Pd_{16}), $[Pd_{16}O_8(OH)_5Cl_3((CH_3)_2AsO_2)_8]$ ($Pd_{16}Cl$), $[Pd_{24}O_{12}(OH)_8((CH_3)_2AsO_2)_{16}]$ (Pd_{24}), and $[Pd_{40}O_{24}(OH)_{16}(CH_3)_2AsO_2)_{16}]$ (Pd_{40}), by using dimethylarsinate as capping group.[6] Very recently, we could isolate the first two examples of cationic palladium(II)–oxo clusters (POCs) by incorporating f-metal ions, $[Pd^{II}_6O_{12}M_8\{(CH_3)_2AsO_2\}_{16}(H_2O)_8]^{4+}$ (M = Ce^{IV}, Th^{IV}),[7a] as well as the mixed-valent palladium(IV/II)–oxoanion $[Pd^{IV}O_6Pd^{II}_6((CH_3)_2AsO_2)_6]^{2-}$.[7b] In 2010, we reported the first discrete polyoxoaurate, $[Au^{III}_4As_4O_{20}]^{8-}$ (Au_4As_4), which was prepared *via* aqueous condensation of *in situ* formed $[Au(OH)_4]^-$ in the presence of AsO_4^{3-} capping groups.[8] Interestingly, in the solid state two Au_4As_4 units are linked by a belt of five sodium counter cations, resulting in the cuboid assembly $\{Na_5(Au_4As_4)_2\}$, which resembles the polyoxo-12-palladate family $\{MPd_{12}X_8\}$. Later a similar strategy was employed to prepare the selenium(IV) analogue $[Au^{III}_4Se_4O_{20}]^{4-}$ (Au_4Se_4), with the arsenate caps being replaced by lone pair containing selenite groups.[9] When reacting Pd^{II} and

[a] *School of Science, Constructor University (formerly Jacobs University), Campus Ring 1, 28759 Bremen, Germany. E-mail: ukortz@constructor.university, u.kortz@jacobs-university.de; Web: https://ukortz.user.jacobs-university.de/*
[b] *Department of Chemistry, BITS Pilani K. K. Birla Goa Campus, 403726 Goa, India*
[c] *Department of Chemistry, Supramolecular Organic and Organometallic Chemistry Centre (SOOMCC), Faculty of Chemistry and Chemical Engineering, Babes-Bolyai University, 400028 Cluj-Napoca, Romania*

† Dedicated to Prof. Michael T. Pope on the occasion of his 90th Birthday.

‡ Electronic supplementary information (ESI) available: Analytical techniques, XRD details, IR and ^{195}Pt NMR spectra, TGA, selected BVS values, bond lengths and mass spectrum. CCDC 2221906, 2221907 and 2249169. For ESI and crystallographic data in CIF or other electronic format see DOI: https://doi.org/10.1039/d3cc00243h

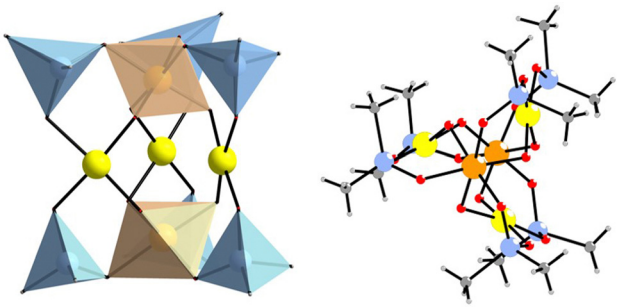

Fig. 1 Combined ball-and-stick/polyhedral representation and Ball-and-stick representation (side view) of **1**. Color code: $\{PtO_6\}$ orange octahedra, $\{(CH_3)_2AsO_2\}$ blue tetrahedra, Au yellow atoms. Pt orange, Au yellow, As sky blue, O red, C grey. Hydrogen atoms omitted for clarity.

Au^{III} ions at the same time with the arsenate capping group, the first fully inorganic, mixed gold–palladium–oxoanion $[NaAu^{III}{}_4Pd^{II}{}_8O_8(AsO_4)_8]^{11-}$ (Au_4Pd_8) could be obtained.[10] Very recently, three more 12-palladate cubes with arsenate capping groups were reported, $[ScO_8Pd_{12}(AsO_4)_8]^{13-}$ and $[MO_8Pd_{12}(AsO_4)_8]^{14-}$ (M = Co^{II}, Cu^{II}).[11] It becomes apparent that the polyoxoplatinate and polyoxoaurate chemistry has been stagnant ever since the reports of the early members (*vide supra*). The research on Pt–Au containing compounds is largely limited to bimetallic nanoparticles, which exhibit excellent catalytic activity.[12] However, to date no polyoxoanion containing both platinum(IV) and gold(III) centers has been reported.

Herein, we report on the first example of a discrete mixed platinum(IV)–gold(III) oxoanion, $[Pt^{IV}{}_2Au^{III}{}_3O_6((CH_3)_2AsO_2)_6]^-$ (**1**, see Fig. 1), which was synthesized in aqueous medium at 80 °C and isolated as a hydrated sodium salt, $Na[Pt^{IV}{}_2Au^{III}{}_3O_6((CH_3)_2AsO_2)_6]\cdot NaCl\cdot NaNO_3\cdot 6H_2O$ (**Na-1**) or a potassium salt, $K[Pt^{IV}{}_2Au^{III}{}_3O_6((CH_3)_2AsO_2)_6]\cdot KCl\cdot KAsO_2(CH_3)_2\cdot 18H_2O$ (**K-1**) in good yield.[13] The polyanion **1** was prepared by reaction of $H_2[Pt(OH)_6]$ with hydrogen tetrachloroaurate $H[AuCl_4]$ in a pH 7 sodium dimethylarsinate (also known as sodium cacodylate, Na-Cac) buffer, resulting in a rapid color change (the initial orange solution color becomes orange-red). It is well known that an acidification of a $[Au(OH)_4]^-$ solution leads to the formation of insoluble $Au(OH)_3$, and that chloride ions do not compete with OH^- for Au^{III} in neutral or slightly alkaline solutions (pH 7.0 to 8.5).[13] In our case, the *in situ* formed tetrahydroxogold(III) ion $[Au(OH)_4]^-$ (or a closely related derivative) reacts smoothly with $[Pt(OH)_6]^{2-}$ in the presence of cacodylate ions, which act as capping groups, thereby terminating the condensation process.

The polyanion **1** possesses a waterwheel structure with two Pt^{IV} ions linked by three square-planar coordinated Au^{III} ions and terminally coordinated by six cacodylate ligands, resulting in an assembly with C_{3h} symmetry (Fig. 1). For **K-1**, the average Au^{III}–O bond lengths are 1.953(9) Å for the oxo ligands and 2.017(9) Å for the oxygen atoms of the cacodylate fragments. Bond valence sum (BVS) calculations showed no protonation for any bridging oxygen atoms (Table S5, ESI‡).[14] The average Au^{III}–O bond lengths in **K-1** (1.986 ± 0.010 Å) are comparable to those in other known gold(III)–oxo complexes, such as the square-planar Au_2O_2 core of $[Au_2\{N_2C_{10}H_7(CH_2CMe_3)\text{-}6\}_2(\mu\text{-}O)_2][PF_6]_2$ (1.976(3) and 1.961(3) Å),[15] the $SrAu_2(CH_3COO)_8$ (1.979 ± 0.008) Å,[16] or the polyoxoaurate Au_4As_4 (1.980 ± 0.023 Å),[8] and quite a bit shorter than the Au–O distance in dimethylgold(III) hydroxide ((2.154 ± 0.148) Å).[17] The Au···Au distance in **K-1** (3.973 ± 0.070 Å) is significantly longer than in Au_4As_4 (3.246 ± 0.024 Å). The Pt–O bond lengths around the octahedrally coordinated Pt centers are quite regular, ranging from 1.960(9) to 2.063(9) Å. The same applies for the sodium salt **Na-1**. The three Au^{III} ions in **1** are located in the same plane and exhibit a slightly distorted square-planar coordination. The oxo ligands bridging to the platinum centers are situated on both sides of this $\{Au_3\}$ plane, while all O–As–O bridges connect a Pt and a Au atom (Fig. 1). In the solid-state lattice of **Na-1**, the polyanions are surrounded by a belt of six Na^+ ions, three NO_3^- ions, and three Cl^- ions, resulting in a supramolecular 2D layer with a hexagonal pattern (Fig. S2, ESI‡).

To complement our solid-state XRD results on **1** with solution studies, we performed ^1H, ^{13}C and ^{195}Pt NMR measurements on **Na-1** and **K-1** redissolved in H_2O/D_2O. The ^1H NMR spectrum of the reference Na-Cac in water exhibits sharp peaks at 4.7 and 1.4 ppm, respectively, corresponding to the protons of the cacodylate methyl groups and crystal water molecules. On the other hand, the ^1H NMR spectrum of **Na-1** exhibits peaks at 2.1 and 1.7 ppm that correspond to the two structurally and hence magnetically inequivalent cacodylate methyl groups (Fig. 2). The ^1H NMR spectrum of **K-1** exhibits three distinct peaks at 2.1, 1.7, and 1.6 ppm, respectively. The two downfield signals belong to **1**, whereas the peak at 1.6 ppm corresponds to the methyl protons of free cocrystallized cacodylate ions. We also investigated the pH stability of polyanion 1 by NMR and the pH-dependent ^1H NMR spectra show that polyanion **1** is stable at pH 2 to 10 (Fig. S4, ESI‡). The ^{13}C NMR spectrum of **Na-1** exhibits peaks at 22.8 and 17.1 ppm that correspond to the two structurally inequivalent cacodylate methyl groups (Fig. 2). The ^{13}C NMR spectrum of Na-Cac exhibits a narrow peak at 17.3 ppm. The ^{13}C NMR spectrum of **K-1** exhibits three distinct sharp peaks (in analogy to its ^1H NMR spectrum) at 22.8, 17.2, and 17.4 ppm corresponding to the methyl groups of the two structurally inequivalent cacodylate methyl groups of **1** and free cocrystallized cacodylate ions, respectively.

Next, we performed ^{195}Pt NMR measurements on **Na-1** and **K-1** redissolved in water. This technique had been applied earlier for the platinum(IV)-containing decavanadate $[H_2Pt^{IV}V_9O_{28}]^{5-}$, exhibiting a clean signal at δ = 3832 ppm.[18] We located the expected singlet for **Na-1** and **K-1** at 3140 and 3142 ppm, respectively (Fig. 3). The corresponding ^{195}Pt NMR signal for the precursor $H_2[Pt(OH)_6]$

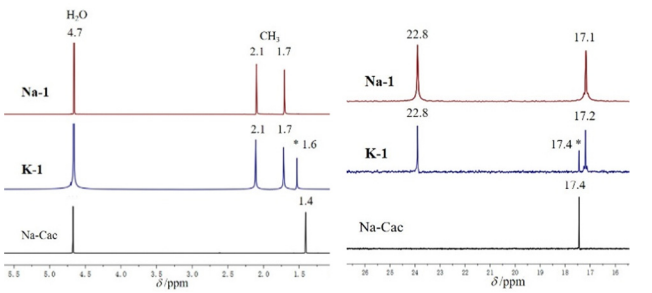

Fig. 2 ^1H (left) and ^{13}C (right) NMR spectra of **Na-1** and **K-1** dissolved in H_2O/D_2O compared to spectra of the sodium cacodylate reference.

appeared more downfield at 3294 ppm. We also performed time and temperature dependent ^{195}Pt NMR measurements on fresh synthesis solutions of **Na-1** (Fig. S5, ESI‡). After stirring at room temperature for 10 min and 40 min there are two peaks at 3316 and 3142 ppm, respectively, corresponding to the reagent $H_2Pt(OH)_6$ and polyanion **1**. However, after heating at 40 °C for 30 min, the spectrum exhibits only a narrow peak at 3141 ppm, indicating that **1** is formed cleanly as the only product during the reaction procedure, suggesting a reaction yield of essentially 100%, which is extremely rare in POM chemistry. The combination of ^{1}H, ^{13}C, and ^{195}Pt NMR is fully consistent with the solid-state structure of **K-1** and **Na-1** and hence provides unequivocal evidence for the presence of polyanion **1** also in solution.

Furthermore, the sodium and potassium salts of polyanion **1** were investigated by ESI-MS in the positive and negative ion modes. In the negative ion mode, signals centered around *m*/*z* 1898.55 were observed for both **Na-1** and **K-1**. These could be clearly assigned to the singly-charged title polyanion $[Pt^{IV}{}_2Au^{III}{}_3O_6((CH_3)_2AsO_2)_6]^-$ (**1**), see Fig. 4. In the positive ion mode spectrum of **Na-1**, a main group of signals was observed centered around *m*/*z* 983.75, corresponding to a doubly-charged species with an elemental composition of $[Na_3Pt_2Au_3O_6(AsO_2(CH_3)_2)_6]^{2+}$ (Fig. S11, ESI‡). The isotope distribution was fully confirmed by comparison of the experimental spectrum to a simulated spectrum. Thus, the ESI-MS spectra of **Na-1** and **K-1** corroborate the solid-state structural analysis and show that polyanion **1** is structurally intact in solution, even under ESI conditions.

We discovered that **Na-1** undergoes a reversible single-crystal-to-single-crystal (SCSC) transformation in the solid state upon rehydration and hydration, where rehydration was achieved by keeping the sample in an atmosphere of water vapor at room temperature and dehydration was achieved by air drying for one day. The polyanion **1** crystallizes in the centrosymmetric space group $P6_3/m$ when in the mother liquor (**Na-1a**), but after air drying for one day, it transforms to the non-centrosymmetric space group $P\bar{6}$ (**Na-1**). The two crystal structures show the exact same polyanion as confirmed by single-crystal XRD, but the unit cell volume shrinks significantly from 2775.2(4) to 2130.9(12) Å^3 upon air-drying for a day, and the packing arrangement is significantly different, because the layer sequence is AAA in **Na-1** and ABA in **Na-1a** (Fig. S3, ESI‡). The structural transformation of **Na-1a** to **Na-1** upon dehydration by air drying was also confirmed by powder-XRD (PXRD) measurements (Fig. 5 and Fig. S12, ESI‡), due to significantly different stacking of the

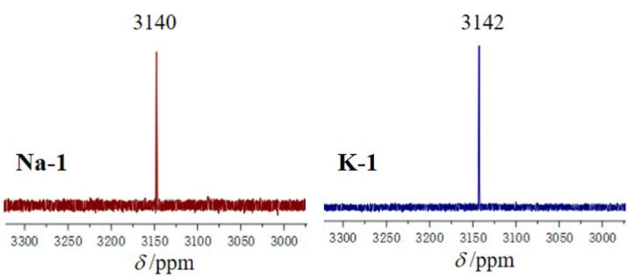

Fig. 3 ^{195}Pt NMR spectra of **Na-1** and **K-1** dissolved in H_2O/D_2O.

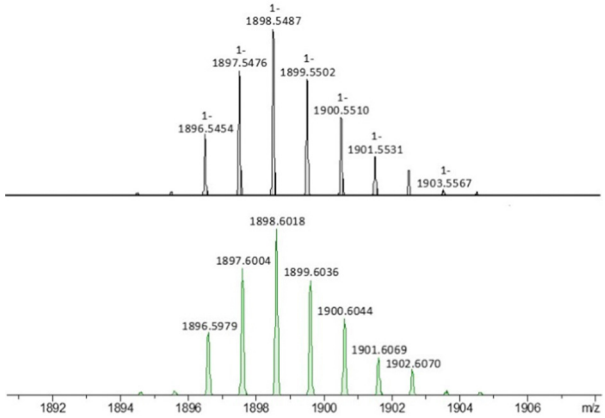

Fig. 4 Simulated ESI-MS spectrum of **Na-1** and **K-1** in negative-ion mode (top) and experimental ESI-MS spectrum (bottom) of the singly-charged polyanion **1** (expanded view).

2-D layers. A pure phase of **Na-1a** is obtained in the crystals in the mother liquor, but after drying in air for one day, a transformation to the new phase **Na-1** occurs. After 2 days, a completely pure phase of **Na-1** is observed. The transformation from **Na-1** to **Na-1a** is fully reversible during a rehydration and dehydration process. Rehydration of **Na-1** in the presence of water vapor at room temperature results in **Na-1a** within half an hour. The rehydration behavior of **Na-1** was also demonstrated by thermogravimetric analysis (TGA) and infrared spectroscopy (FT-IR) on **Na-1** (Fig. S7 and S9, ESI‡). Single-crystal-to-single-crystal (SCSC) transformations constitute solid-state transitions induced by an external stimulus, such as light, heat, guest, or mechanochemical forces.[19] While SCSC transformations in metal–organic frameworks (MOFs) and coordination polymers (CPs) are well-documented, examples for discrete complexes remain scarce. To our knowledge, only five other thermally-induced processes in POM structures have been described, involving high-, room- and low- temperature polymorphic transitions[20] or structural variations by dehydration.[21]

We have synthesized and structurally characterized the first discrete mixed gold–platinum–oxoanion $[Pt^{IV}{}_2Au^{III}{}_3O_6((CH_3)_2AsO_2)_6]^-$ (**1**) by using simple one-pot open-beaker techniques. The ^{195}Pt NMR spectrum of redissolved solid **1** in water demonstrates solution stability, which provides much potential

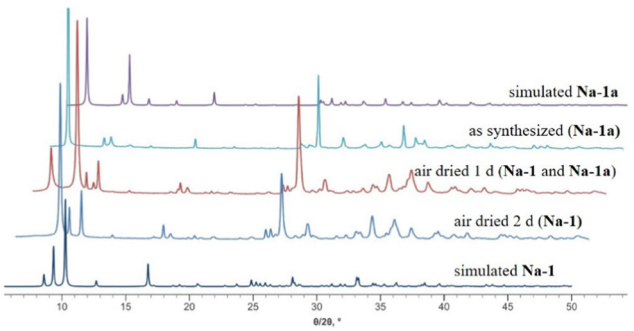

Fig. 5 Experimental and simulated PXRD patterns of **Na-1a** and **Na-1** during a dehydration process by air drying (simulated diffraction patterns derived from single-crystal data).

for further applications of **1** in catalysis and biomedicine. The reversible single-crystal-to-single-crystal transformation of **Na-1a** to **Na-1** upon dehydration and rehydration is of particular interest, as concern solid state applications (sorption etc). The title polyanion **1** merges the areas of polyoxoplatinate and polyoxoaurate chemistry and pushes the area of polyoxo-noble-metalate chemistry to a higher synthetic and analytical level. Further studies in this area are ongoing.

U. K. thanks the German Research Council (DFG, KO 2288/26-1 and KO 2288/29-1) and Constructor University (formerly Jacobs University) for support. J. Z. sincerely acknowledges CSC (China Scholarship Council) for a doctoral fellowship.

Conflicts of interest

There are no conflicts to declare.

Notes and references

1 (*a*) J. Berzelius, *Poggendorff's Ann. Phys.*, 1826, **6**, 369–380; (*b*) M. T. Pope, Y. Jeannin and M. Fournier, *Heteropoly and Isopoly Oxometalates*, Springer-Verlag, Berlin Heidelberg, 1983; (*c*) M. T. Pope, M. Sadakane and U. Kortz, *Eur. J. Inorg. Chem.*, 2019, 340–342.

2 (*a*) M. T. Pope and A. Müller, *Polyoxometalate Chemistry: From Topology via Self-Assembly to Applications*, Kluwer Academic Publishers, Dordrecht, Netherlands, 2001; (*b*) S. S. Wang and G. Y. Yang, *Chem. Rev.*, 2015, **115**, 4893–4962; (*c*) M. R. Horn, A. Singh, S. Alomari, S. Goberna-Ferrón, R. Benages-Vilau, N. Chodankar, N. Motta, K. Ostrikov, J. MacLeod, P. Sonar, P. Gomez-Romero and D. Dubal, *Energy Environ. Sci.*, 2021, **14**, 1652–1700; (*d*) N. I. Gumerova and A. Rompel, *Nat. Rev. Chem.*, 2018, **2**, 0112.

3 (*a*) J. C. Goloboy and W. G. Klemperer, *Angew. Chem., Int. Ed.*, 2009, **48**, 3562–3564; (*b*) P. Putaj and F. Lefebvre, *Coord. Chem. Rev.*, 2011, **255**, 1642–1685; (*c*) I. A. Weinstock and A. Müller, *Isr. J. Chem.*, 2011, **51**, 176–178; (*d*) N. V. Izarova, M. T. Pope and U. Kortz, *Angew. Chem., Int. Ed.*, 2012, **51**, 9492–9510; (*e*) P. Yang and U. Kortz, *Acc. Chem. Res.*, 2018, **51**, 1599–1608; (*f*) L. Rocchigiani and M. Bochmann, *Chem. Rev.*, 2021, **121**, 8364–8451.

4 (*a*) M. Pley and M. S. Wickleder, *Angew. Chem., Int. Ed.*, 2004, **43**, 4168–4170; (*b*) A. Rajan, M. E. Mahmoud, F. Wang, S. Bhattacharya, A. S. Mougharbel, X. Ma, A. B. Müller, T. Nisar, D. H. Taffa, J. M. Poblet, N. Kuhnert, V. Wagner, M. Wark and U. Kortz, *Inorg. Chem.*, 2022, **61**, 11529–11538.

5 E. V. Chubarova, M. H. Dickman, B. Keita, L. Nadjo, F. Miserque, M. Mifsud, I. W. C. E. Arends and U. Kortz, *Angew. Chem., Int. Ed.*, 2008, **47**, 9542–9546.

6 (*a*) S. Bhattacharya, U. Basu, M. Haouas, P. Su, M. F. Espenship, F. Wang, A. Sole-Daura, D. H. Taffa, M. Wark, J. M. Poblet, J. Laskin, E. Cadot and U. Kortz, *Angew. Chem., Int. Ed.*, 2021, **60**, 3632–3639; (*b*) S. Bhattacharya, X. Ma, A. S. Mougharbel, M. Haouas, P. Su, M. F. Espenship, D. H. Taffa, H. Jaensch, A. J. Bons, T. Stuerzer, M. Wark, J. Laskin, E. Cadot and U. Kortz, *Inorg. Chem.*, 2021, **60**, 17339–17347.

7 (*a*) S. Bhattacharya, A. Barba-Bon, T. A. Zewdie, A. B. Müller, T. Nisar, A. Chmielnicka, I. A. Rutkowska, C. J. Schürmann, V. Wagner, N. Kuhnert, P. J. Kulesza, W. M. Nau and U. Kortz, *Angew. Chem., Int. Ed.*, 2022, **61**, e202203114; (*b*) X. Ma, S. Bhattacharya, T. Nisar, A. B. Müller, V. Wagner, N. Kuhnert and U. Kortz, *Chem. Commun.*, 2023, **59**, 904–907.

8 N. V. Izarova, N. Vankova, T. Heine, R. Ngo Biboum, B. Keita, L. Nadjo and U. Kortz, *Angew. Chem., Int. Ed.*, 2010, **49**, 1886–1889.

9 Y. Xiang, N. V. Izarova, F. Schinle, O. Hampe, B. Keita and U. Kortz, *Chem. Commun.*, 2012, **48**, 9849–9851.

10 N. V. Izarova, A. Kondinski, N. Vankova, T. Heine, P. Jäger, F. Schinle, O. Hampe and U. Kortz, *Chem. – Eur. J.*, 2014, **20**, 8556–8560.

11 P. Yang, M. Elcheikh Mahmoud, Y. Xiang, Z. Lin, X. Ma, J. H. Christian, J. K. Bindra, J. S. Kinyon, Y. Zhao, C. Chen, T. Nisar, V. Wagner, N. S. Dalal and U. Kortz, *Inorg. Chem.*, 2022, **61**, 18524–18535.

12 (*a*) S. Zhou, G. S. Jackson and B. Eichhorn, *Adv. Funct. Mater.*, 2007, **17**, 3099–3104; (*b*) R. P. Doherty, J.-M. Krafft, C. Méthivier, S. Casale, H. Remita, C. Louis and C. Thomas, *J. Catal.*, 2012, **287**, 102–113; (*c*) N. Biswakarma, D. Dowerah, S. D. Baruah, P. J. Sarma, N. K. Gour and R. C. Deka, *Mol. Catal.*, 2021, **515**, 111910.

13 (*a*) G. Jander and G. Krien, *Z. Anorg. Allg. Chem.*, 1960, **304**, 154–163; (*b*) P. G. Jones, H. Rumpel, E. Schwarzmann and G. M. Sheldrick, *Acta Crystallogr., Sect. B: Struct. Crystallogr. Cryst. Chem.*, 1979, **35**, 1435–1437; (*c*) D. Vlassopoulos and S. A. Wood, *Geochim. Cosmochim. Acta*, 1990, **54**, 3–12.

14 I. D. Brown and D. Altermatt, *Acta Crystallogr., Sect. B*, 1985, **41**, 244–247.

15 M. A. Cinellu, G. Minghetti, M. V. Pinna, S. Stoccoro, A. Zucca, M. Manassero and M. Sansoni, *J. Chem. Soc., Dalton Trans.*, 1998, 1735–1741.

16 P. G. Jones, *Acta Crystallogr., Sect. C: Cryst. Struct. Commun.*, 1984, **40**, 804–805.

17 (*a*) M. G. Miles, G. E. Glass and R. S. Tobias, *J. Am. Chem. Soc.*, 1966, **88**, 5738–5744; (*b*) G. E. Glass, J. H. Konnert, M. G. Miles, D. Britton and R. S. Tobias, *J. Am. Chem. Soc.*, 1968, **90**, 1131–1138; (*c*) S. J. Harris and R. S. Tobias, *Inorg. Chem.*, 1969, **8**, 2259–2264.

18 (*a*) U. Lee, H. C. Joo, K. M. Park, S. S. Mal, U. Kortz, B. Keita and L. Nadjo, *Angew. Chem., Int. Ed.*, 2008, **47**, 793–796; (*b*) S. Dugar, N. V. Izarova, S. S. Mal, R. Fu, H.-C. Joo, U. Lee, N. S. Dalal, M. T. Pope, G. B. Jameson and U. Kortz, *New J. Chem.*, 2016, **40**, 923–927.

19 (*a*) A. Chaudhary, A. Mohammad and S. M. Mobin, *Cryst. Growth Des.*, 2017, **17**, 2893–2910; (*b*) F. Hu, X. Bi, X. Chen, Q. Pan and Y. Zhao, *Chem. Lett.*, 2021, **50**, 1015–1029; (*c*) E. Fernandez-Bartolome, A. Martinez-Martinez, E. Resines-Urien, L. Piñeiro-Lopez and J. Sanchez Costa, *Coord. Chem. Rev.*, 2022, **452**, 214281.

20 (*a*) L. -Z. Zhang, W. Gu, Z. Dong, X. Liu and B. Li, *CrystEngComm*, 2008, **10**, 1318–1320; (*b*) S. Reinoso, M. H. Dickman, A. Praetorius and U. Kortz, *Acta Crystallogr.*, 2008, **E64**, m614–165.

21 (*a*) A. Iturrospe, L. S. Felices, S. Reinoso, B. Artetxe, L. Lezama and J. M. Gutierrez-Zorrilla, *Cryst. Growth Des.*, 2014, **14**, 2318–2328; (*b*) D. Barats-Damatov, L. J. W. Shimon, Y. Feldman, T. Bendikov and R. Neumann, *Inorg. Chem.*, 2015, **54**, 628–634; (*c*) L. Fernandez-Navarro, A. Iturrospe, S. Reinoso, B. Artetxe, E. Ruiz-Bilbao, L. S. Felices and J. M. Gutierrez-Zorrilla, *Cryst. Growth Des.*, 2020, **20**, 3499–3509.